A BLOCK STRUCTURED BASED METHOD FOR THE FLOW PREDICTION OVER LOW REYNOLDS NUMBERS MULTI-ELEMENT AIRFOILS(*)

F.Wilquem[1], C.Passelecq[1] and G.Degrez[2]

(1) Faculté Polytechnique de Mons, Fluid Mechanics Dept., Rue de Houdain 9, 7000 Mons (Belgium)
(2) von Karman Institute for Fluid Dynamics, Aeronautics Dept., Chaussée de Waterloo 72, 1640 Rhode-St-Genèse (Belgium)

Summary

This paper describes and evaluates a general two-dimensional block structured grid generation technique which is coupled with a high resolution incompressible Euler/Navier-Stokes solver to simulate steady low Reynolds number flows around multi-element airfoils configurations. The grids are generated using an object-oriented algorithm which automates several stages in the decomposition of the domain into non-overlapping topologically rectangular regions. The solution procedure uses a finite-volume formulation and takes advantage of some recent advances in the pseudo-compressibility concept, namely the use of flux-difference to upwind evaluate the convective fluxes. The effects of turbulence on the mean flow are described by means of the Baldwin-Lomax model. The discretized equations are marched in time to steady-state using various implicit procedures. The Williams wing-flap configuration with 10° and 30° flap deflections is chosen as a reference test case. The surface pressure distributions computed in inviscid conditions at zero incidence are found to be in good agreement with Karman-Trefftz mapping and panel based methods. Additional tests are carried out with success in the turbulent regime up to chord-based Reynolds numbers of 1.2 million, thus demonstrating the efficiency of the numerical scheme.

Introduction

With the progress achieved in numerical algorithms and also in the field of computer technology, computing flow field around complex aerodynamic configurations is now possible. In order to achieve optimum designs, new tools for rapid and efficient analysis of high-lift configurations are required. Computational fluid dynamics offers great promises as a tool which provides valuable insight into the flow phenomena associated with high-lift system performances. Nevertheless, the generation of acceptable body-fitted grids is often quite a burden. The fundamental problem with grid generation for aircraft-like shapes is that each aerodynamic component of the configuration has its own natural structure. However, these structures are usually incompatible with each other. This has lead to the idea of generating grids whose topology is locally consistent with each component but with some global means of connecting the grids. This naturally leads to the concept of block structured grids.

Multi-element configurations present a large number of challenging problems for the numericists; these includes boundary layer separation, wake flows, transition effects and of course complex geometries. In take-off and landing flow conditions, Mach number effects are negligible mainly because of the low velocity level, except maybe in the leading edge area of the main airfoil. Consequently, the flow field may be modelled using the incompressible form of the Reynolds averaged Navier-Stokes equations.

Low Reynolds flows about high-lift systems have been investigated by a number of authors. Recent papers on the topic include the use of structured patched grids[1,2], overlapping Chimera grids[3,4,5] and unstructured grids[6]. Turbulence effects are generally modelled using the Baldwin-Lomax[1,3] model, the Baldwin-Barth model[3,4], the

Spalart-Allmaras model[5] or various versions of the k-ε model[1,2].

The intent of the present work is to describe and evaluate a general 2D block structured grid generation technique which is coupled with a high resolution incompressible Euler/Navier-Stokes solver to simulate steady low Reynolds number flows around multi-element airfoils configurations. A particular accent is laid on the efficiency of implicit time integration procedures through the evaluation of single and multi-step(s) strategies.

Grid Generation

Generating an appropriate grid around a practical multi-element geometry can be a difficult task. In particular, the construction of a single grid system that covers the entire flow field can be really hard or even impossible to realize. By dividing the domain into non-overlapping topologically rectangular regions, a local structured grid may be generated within each block. Because continuity of location of grid points is not required at block boundaries, grids can be generated in each block separately without any restriction. One of the major advantages of using block structured grids obviously lies in the simplification of the grid generation procedure but this approach also easily allows the grid refinement in zones where a fine resolution is required. The sub-regions grids are generated either by the solution of partial differential equations (of hyperbolic or elliptic nature) or by algebraic and NURBS (Non-Uniform Rational B-Spline) interpolation.

The grids are generated using an object-oriented algorithm which automates several stages in the decomposition of the domain into non-overlapping topologically rectangular regions. The whole grid generation process is accomplished in 11 steps, as described in fig. 1. Basically, the object-oriented concept integrated within the code allows to give the user freedom and flexibility to act at any time at a given step without any interaction with the other ones; the grid generation process then further automatically proceeds using the latest available data.

The airfoil geometry is modelled using NURBS interpolation. This technique which has for instance been used with success by Yu and al. [7] allows to parametrize the geometry boundary C(t) as

$$C(t) = \frac{\sum_{i=0}^{n} w_i \; P_i \; N_{i,k}(t)}{\sum_{i=0}^{n} w_i \; N_{i,k}(t)}$$

with

$$N_{i,1}(t) = 1 \quad \text{if } v_i \le t \le v_{i+1}$$
$$= 0 \quad \text{elsewhere}$$

and

$$N_{i,k}(t) = \frac{(t - v_i)\, N_{i,k-1}(t)}{v_{i+k-1} - v_i} + \frac{(v_{i+k} - t)\, N_{i+1,k-1}(t)}{v_{i+k} - v_{i+1}}$$

where P is the control nodes vector and w is its associated weighting vector; v_i is the i-th component of the normalized nodal vector associated to curve C. Its dimension t_{max} is given as $t_{max} = n - k + 2$ where n represents the number of segments on the original curve and k is the NURBS order (k must be at least equal to 2).

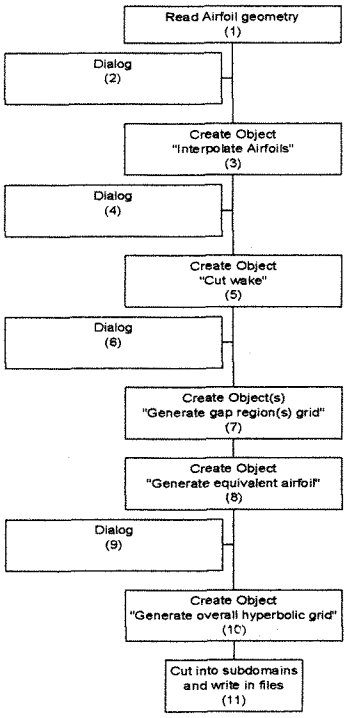

FIGURE 1 - grid generation strategy using the object-oriented concept.

The blocking strategy around the Williams wing-flap configuration is shown in fig. 2. The gap region is first modelled by considering an

equivalent airfoil whose geometry is defined in an automatic way and is further gridded using NURBS 2D interpolation extending the above formula as

$$S(t,t^*) = \frac{\sum_{i=0}^{n} \sum_{j=0}^{m} w_{i,j} \; P_{i,j} \; N_{i,p}(t) \, N_{i,q}(t^*)}{\sum_{i=0}^{n} \sum_{j=0}^{m} N_{i,p}(t) \, N_{i,q}(t^*)}$$

An hyperbolic-type grid is then generated around the equivalent airfoil and the final grid is splitted into 8 blocks, including the gap region. A partial view of the resulting grid about the airfoils with 30° flap deflection is shown in fig. 3.

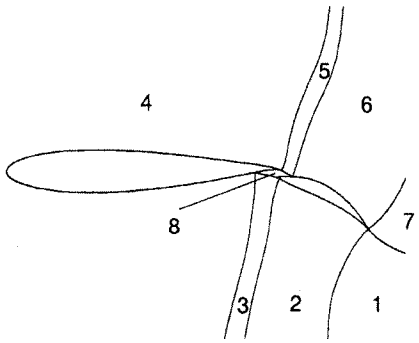

FIGURE 2 - blocking strategy about the two-element Williams airfoil with 30° flap deflection.

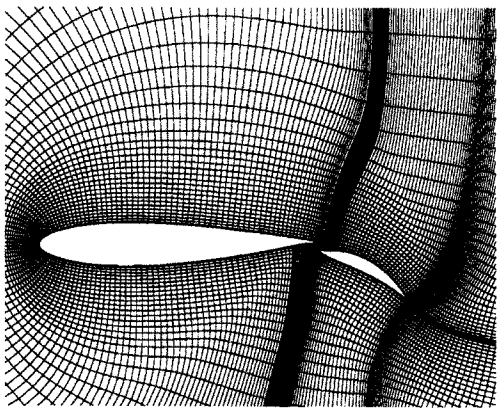

FIGURE 3 - partial view of the 8 blocks grid about the two-element Williams airfoil with 30° flap deflection in inviscid flow conditions.

Mathematical Model

Mean Flow Equations

Coupling the continuity and momentum equations with the artificial compressibility formulation as developed by Chorin[8], the Reynolds averaged Navier-Stokes equations which describe two-dimensional steady incompressible flows are given by

$$\frac{1}{\rho}\frac{\partial p}{\partial t} + \beta \frac{\partial U_i}{\partial x_i} = 0$$

$$\rho\left(\frac{\partial U_i}{\partial t} + \frac{\partial (U_i U_j)}{\partial x_j}\right) = -\frac{\partial p}{\partial x_i} + \frac{\partial}{\partial x_j}\left(\mu \frac{\partial U_i}{\partial x_j} - \rho \overline{u_i u_j}\right)$$

where U_i denotes the mean velocities and u_i the corresponding fluctuating velocities in x_i directions. p stands for mean static pressure and μ and ρ for molecular viscosity and density of the fluid, respectively; overbars indicate time-averaged quantities.

Turbulence Model

The Reynolds-averaging of the Navier-Stokes equations introduces a further set of unknowns, the so-called Reynolds stresses. For the very large majority of numerical methods, these stresses are related to the mean flow quantities through the introduction of additional relations which describe the turbulence model.

$$-\rho \overline{u_i u_j} = \mu_t \frac{\partial U_i}{\partial x_j}$$

In the present method, turbulence closure is provided by the Baldwin-Lomax algebraic model[9]. It is a two-layer model which determines the turbulent viscosity in an inner and outer layer which are subsequently matched.

$$\begin{aligned} \mu_t &= \mu_{inner} \quad \text{if } y \le y_{crossover} \\ &= \mu_{outer} \quad \text{if } y > y_{crossover} \end{aligned}$$

where $y_{crossover}$ is the first point at which μ_{inner} exceeds μ_{outer}. In the present work, the viscosity switching is only effective as far as $y^+ \le 35$ in order to avoid it to occur too far from the wall. In

addition, the ratio of the resulting turbulent viscosity to the laminar one is limited to 1000 to prevent spurious high viscosities to appear within the flow field and consequently alter the convergence process.

In order to overcome the extremely fine grids required to model boundary layers accurately down to the wall, the following law of the wall model is used to evaluate the shear stresses at wall boundaries.

$$u^+ = \frac{1}{0.435} \ln (1.01 + 9y^+)$$

Indeed, the cell Reynolds number Re_c may be defined at the walls as $Re_c = u^- y^-$. Once Re_c is known, the two above relations may be curve fitted to deduce y^- and further proceed to evaluate the wall shear stress τ_w through the definition of u^-. This approach has already been used with success by Turner and Jennions[10] and allows to drop the Van Driest damping terms within the original formulation.

The formulation of Granville[11] for the evaluation of constants appearing within the model is used to better take the effect of varying pressure gradients into account.

The effect of transition to turbulence is simulated using the Klebanoff intermittency factor and setting μ_t equal to zero everywhere in a profile for which the maximum tentatively computed value of μ_t is less than a threshold value, as given in the original Baldwin and Lomax paper[9].

$$\mu_t = 0 \quad \text{if } (\mu_t)_{max} < 14\mu$$

Boundary Conditions

An extended characteristic-based method is used to evaluate the numerical boundary conditions in a consistent way. The starting point is a consistency condition for the inviscid numerical flux function. The unknows at a boundary are determined such that the flux function based on the boundary and first adjacent solution vectors lead to fluxes which satisfy the physical boundary conditions. More details may be found in Wilquem and Degrez[12].

The partitionning of the computational domain in non-overlapping subdomains introduces internal boundaries corresponding to the interfaces between adjacent blocks. Because the computations are carried out separately in each block, a block adjacency relationship must be defined in a connectivity array for a correct evolution of the solution. The data structure required to describe this connectivity in particular includes two layers of ghost cells which surround each of the blocks sides; the second layer is needed at higher accuracy orders because of the MUSCL extrapolation.

The multiblock strategy developed in the frame of this work can either deal with direct connecting or patched block interfaces. Consequently, great care must be exercised in treating interface points to transfer the information accurately. The continuity of the state vector is enforced along the boundaries shared by two direct connecting blocks. In these conditions, the MUSCL extrapolation as well as the evaluation of the velocity gradients is simply extended through the connectivity array across the interblock boundaries. In the frame of patched blocks, the fluxes computation is carried out for each interface segments; in these circumstances, no extension is performed in the evaluation of the velocity gradients.

The update of the interface cells is performed in an explicit way once each iteration. Computations can then proceed in each block without the need for further information from adjacent blocks. In addition, the method also allows multiple boundary conditions per block side, which significantly increases the flexibility of the code.

Numerical Solution Procedure

The numerical solution procedure is based on a conservative cell-centered finite volume method. A second order accurate central difference scheme is used to discretize the diffusive fluxes whereas the convective fluxes are approximated by the Roe flux-difference splitting scheme. High order space accuracy is achieved using the MUSCL variable extrapolation method. The discretized equations are linearized locally and integrated implicitly in time following a time-marching approach.

Performing an implicit time integration, the governing equations may be rewritten in the following standard form

$$\frac{\Delta Q^n}{\Delta t} = - R^{n+1}$$

where $\Delta Q^n = Q^{n+1} - Q^n$ represents the incremental change in the cell-centered values of the solution vector Q between time levels n and n+1. The residual vector R^{n+1} is linearized in time about the n-th time level as

$$R^{n+1} \approx R^n + \left(\frac{\partial R}{\partial Q} \right)^n \Delta Q^n$$

which results in

$$\left(\frac{I}{\Delta t} + \frac{\partial R}{\partial Q} \right)^n \Delta Q^n = - R^n$$

or, in compact form

$$\left(\frac{I}{\Delta t} + J_R \right)^n \Delta Q^n = J_F \, \Delta Q^n = - R^n$$

where J_R is referred to as the real jacobian of the residuals and J_F is its augmented counterpart. The above relation represents the system of simultaneous linear equations which has to be solved for ΔQ^n at each time step of the integration process. In a majority of CFD applications, because of the large and poorly conditionned properties of the coefficient matrices, the system must be solved in an iterative way.

Both single and multi-step(s) strategies are tested in the frame of this work. Remembering the general form of an iterative solution technique

$$\tilde{J}_F \, \Delta Q^{n,k+1} = - R^n + (\tilde{J}_F - J_F) \, \Delta Q^{n,k}$$

where $\tilde{J}_F$ is the augmented preconditionning matrix and k is the inner iteration counter, a m-step scheme consists in performing m inner iterations per time step. Starting from the initial approximation $\Delta Q^{n,0} = 0$, the single step scheme does not require the evaluation of the jacobian matrices which are particularly hard to compute in the frame of the Roe flux-difference splitting explicit operator. In contrast, multi-steps schemes, evidently more expensive per time step, may be expected to significantly increase the convergence rate of the non-linear iterative process and thus be able to reduce the total CPU time to reach non-linear full convergence. The symmetric point Gauss-Seidel approximate factorization is used as a preconditionning matrix. It is basically a two-steps procedure which is equivalent to a lower Gauss-Seidel sweep followed by an upper one.

At this stage, it is important to note that the accuracy of the steady state solution is entirely controlled by R^n. Consequently, the jacobian J_R may be substituted by some approximation which may unfortunately have some adverse effects on the non-linear convergence process. In the present work, J_R may either be estimated analytically using the Yoon and Jameson approximation[13] or numerically through finite-difference evaluations of the $J_R \, \Delta Q^{n,k}$ product, that is

$$J_R \, \Delta Q^{n,k} \approx \frac{R (Q^n + \varepsilon \, \Delta Q^{n,k}) - R (Q^n)}{\varepsilon}$$

for a forward first-order approximation and

$$J_R \, \Delta Q^{n,k} \approx \frac{R (Q^n + \varepsilon \, \Delta Q^{n,k}) - R (Q^n - \varepsilon \, \Delta Q^{n,k})}{2\varepsilon}$$

for a central second-order approximation. The two latter approximations, which belong to the so-called jacobian-free methods, are a particularly interesting way to go in situations where the Yoon and Jameson approximation is too bad. A key issue in using jacobian-free methods is the proper choice of ε. Following the recommendations of Issman and Degrez[14], a fixed $\varepsilon = 10^{-5}$ is chosen.

Finally, in an attempt to further accelerate the iterative process, the GMRES algorithm[15] may be used in combination with the various multi-steps strategies. Originally designed to iteratively solve linear systems with non-symmetric coefficient matrices, the GMRES method seeks for an approximate solution $\Delta Q^{n,m}$ of the form

$$\Delta Q^{n,m} = \Delta Q^{n,0} + \sum_{k=1}^{m} z^{n,k}$$

where the vector $z^{n,k}$ lies in the Krylov subspace K (J_F, r_0, m) defined by the matrix J_F, the unit vector $w_1 = r_0 / \gamma$ ($r_0 = - R^n - J_F \, \Delta Q^{n,0}$; $\gamma = \| r_0 \|$) and the

size of the Krylov subspace m. This way of solving will converge in the fastest manner as far as each successive iterate $z^{n,k}$ minimizes the residual norm $\|r_k\|$ over the Krylov subspace.

The relative efficiency of different combinations of the previously described solution strategies and jacobian approximations is discussed within the results section.

Results

The Williams wing-flap configuration with 10° and 30° flap deflections is chosen as reference test cases. Conceptually, a global C-type grid consisted of 18070 cells and a sequence of 8 blocks is constructed. Fig. 4 and fig. 5 show the comparison of the computed surface pressure distributions about the airfoils at zero incidence and in inviscid conditions with the conformal mapping method of Williams[16] and the panel method of Coussement[17].

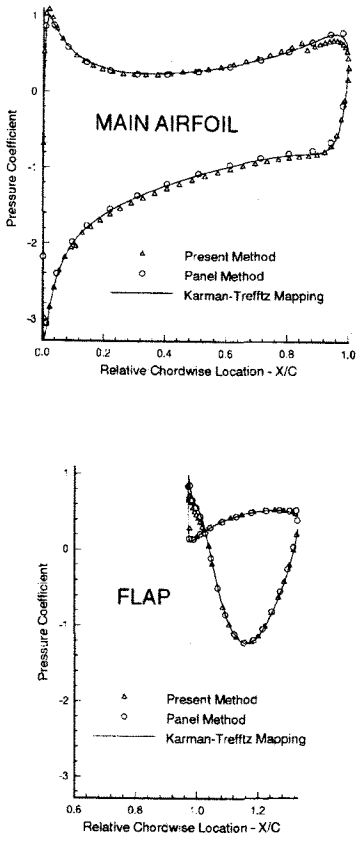

FIGURE 4 - surface pressure distribution about the two-element Williams airfoil with 10° flap deflection in inviscid flow conditions for $\alpha = 0°$.

Although some deviations (as the jump in the pressure coefficient distribution on the main airfoil in fig.4) may be observed because of an insufficient grid quality in the region of the gap, all methods compare quite well. The corresponding predicted lift and drag coefficients for 10° and 30° flap configuration are given in tables 1a and 1b. The agreement between the exact and predicted values is good.

	Williams	Present Method
$C_{L,\ main\ airfoil}$	1.69	1.75
$C_{L,\ flap}$	0.34	0.34
$C_{D,\ main\ airfoil}$	-0.09	-0.06
$C_{D,\ flap}$	0.09	0.09

TABLE 1a - exact and predicted inviscid lift (C_L) and drag (C_D) coefficients about the Williams configuration with 10° flap at zero incidence.

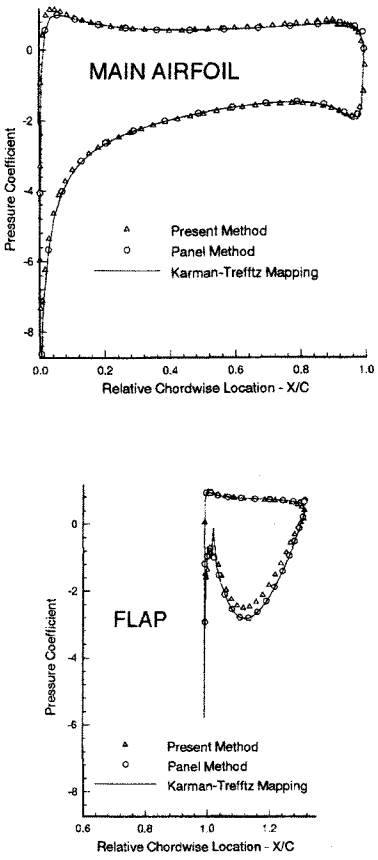

FIGURE 5 - surface pressure distribution about the two-element Williams airfoil with 30° flap deflection in inviscid flow conditions for $\alpha = 0°$.

From a theoretical point of view, the drag coefficient should normally be zero in inviscid

conditions, whatever the airfoil configuration is. Practically, non zero numerical values are due to artificial dissipation as well as truncation errors in the fluxes approximations.

	Williams	Present Method
$C_{L,\ main\ airfoil}$	2.91	2.97
$C_{L,\ flap}$	0.83	0.75
$C_{D,\ main\ airfoil}$	-0.38	-0.29
$C_{D,\ flap}$	0.38	0.36

TABLE 1b - exact and predicted inviscid lift (C_L) and drag (C_D) coefficients about the Williams configuration with 30° flap at zero incidence.

The corresponding convergence histories are shown in fig. 6 by the rms value over the entire field of the u-velocity residual. In both cases, computations have been carried out with CFL=1 using the single step procedure in which the jacobian matrices are reevaluated only each 10 iterations. In these conditions, 3000 iterations and a few CPU hours on a Pentium P90 are required to obtain a 5-order magnitude reduction in velocity residuals.

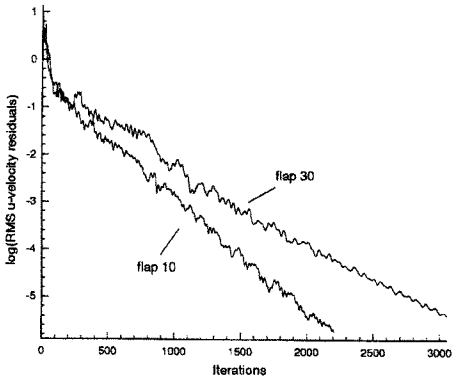

FIGURE 6 - convergence histories for the Williams wing-flap configuration at zero incidence in inviscid conditions for 10° and 30° flap deflection.

To evaluate the effect of the various implicit schemes on non-linear convergence, the viscous turbulent flow over the Williams wing-flap configuration with 10° flap deflection is computed for a chord-based Reynolds number of 1.2 million at zero incidence. The viscous grid is composed of 8 blocks containing 18319 cells with an initial spacing off the solid surfaces of 0.0003 chord to yield a y^+ of approximatively 30-50 using the law of the wall. The outer boundary of the computed domain is 20 chord lengths from the airfoils.

Fig. 7 shows the predicted velocity contours computed using the 10-steps scheme where the effect of the real jacobian on ΔQ^n is evaluated by means of a forward first-order finite difference approximation. Full convergence is achieved within 2000 iterations on a Pentium P90. The block boundaries, shown as dark lines, are transparent to the velocity magnitude contours, indicating a consistent treatment of the interface conditions. In this case, no separation is found on the upper side of the flap.

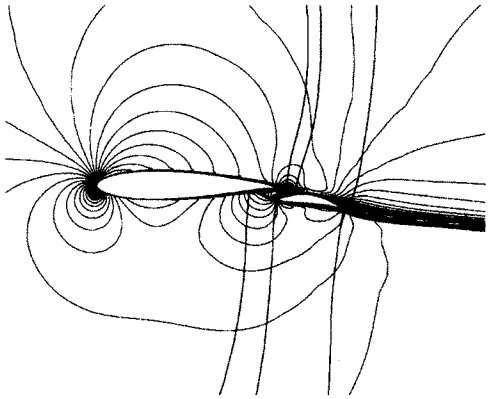

FIGURE 7 - velocity magnitude contours about the two-element Williams configuration with 10° flap deflection for Re = 1.2 million and $\alpha = 0°$.

The corresponding total pressure contours are shown in fig. 8. and demonstrate the development of the boundary layers. The flow field consists of a very thin boundary layer above the main airfoil and is followed by a region of an inviscid core flow which is limited by the viscous region produced by the wakes of each of the airfoils.

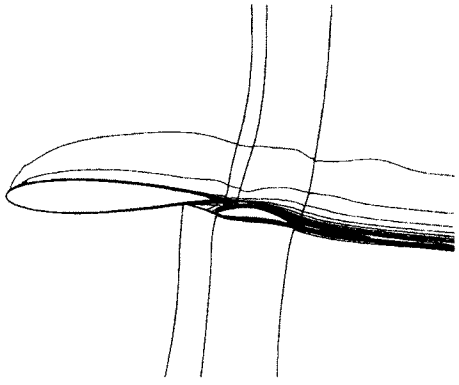

FIGURE 8 - total pressure contours about the two-element Williams airfoil with 10° flap deflection for Re = 1.2 million and $\alpha = 0°$

Seven differents combinations of the solution strategies and jacobian approximations described in the numerical solution procedure section, as indicated in table 2 and subsequently referred to as schemes A to G have been tested. A comparison of the number of iterations and relative CPU time required to obtain a 5-order magnitude reduction in velocity residuals for these various combinations is listed in table 3.

Scheme	Characteristics
A	1-step, jacobians reevaluated each 10 iter.
B	10-steps, Yoon-Jameson
C	10-steps, 1st order forward JFNI
D	10-steps, 2nd order central JFNI
E	10-steps, Yoon-Jameson, GMRES
F	10-steps, 1st order forward JFNI, GMRES
G	10-steps, 2nd order central JFNI, GMRES

TABLE 2 - list of schemes tested for the flow computation about the Williams configuration with 10° flap for Re = 1.2 million at zero incidence.

The corresponding convergence histories are plotted in fig. 9. All cases are computed using CFL=1.0. For the very large majority of schemes investigated, the convergence history locally depicts an oscillatory behavior which correspond to maximum velocity residuals located in the vicinity of the gap region. This phenomenom may probably be understood as a grid effect due to the hyperbolic grid generation technique which forces the grid lines to be orthogonal along the surfaces even in concave regions where it should maybe be better not to force it. At this stage, a comparison of the efficiency of various domain decomposition strategies seems necessary to confirm this hypothesis and will be included in a further study.

Scheme	Iterations	relative CPU
A	7381	1.00
B	> 8000	-
C	7372	2.01
D	7369	2.98
E	> 8000	-
F	1940	0.73
G	1938	1.25

TABLE 3 - number of iterations and relative total CPU time required to obtain a 5-order magnitude reduction in the velocity residuals for the flow about the Williams configuration with 10° flap for Re = 1.2 million at zero incidence.

The single step scheme in which the jacobians are evaluated using the Yoon and Jameson approximation and are updated each 10 iterations here serves as a reference test scheme; its relative CPU time is consequently set to 1. For all multi-steps schemes tested, the treshold value used to stop the linear iterative process and defined as the reduction in residuals within the linear solver was set to 0.01 with a maximum of 10 inner iterations.

Table 3 indicates that net savings of about 27 % in terms of computational cost may be achieved by using the multi-steps schemes instead of single-step ones as far as the accuracy of the jacobian evaluation is high enough to avoid inference with the non-linear convergence behavior. Regarding fig. 9, the Yoon-Jameson approximation (scheme B) clearly appears to be particularly indequate, at least in the frame of the test cases investigated. A second order central finite difference approximation of the $J_R \Delta Q^n$ product (scheme D), although evidently more accurate than a first order forward one (scheme C), does not lead to an increased convergence rate but appears to be a much more time consuming approach.

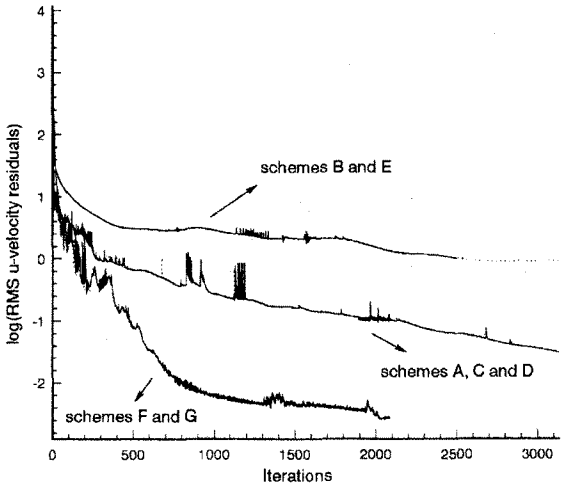

FIGURE 9 - convergence histories for the flow about the two-element Williams airfoil with 10° flap deflection for Re = 1.2 million and $\alpha = 0°$.

The use of the GMRES algorithm within the multi-steps formulation has also been investigated in cases for which the maximum Krylov subspace dimension is limited to 10. Coupled with a first-order forward finite difference approximation of the $J_R \Delta Q^n$ product, the overall scheme (named as F) appears to be particularly efficient. The poor

performances of scheme E confirms the bad effect of the Yoon and Jameson approximation on the non-linear convergence which cannot be enhanced using GMRES. Again, the use of a second-order central evaluation of the $J_R \Delta Q^n$ product (scheme G) appears more time consuming. All converged solutions obtained using schemes A to G were found to be identical within 1% accuracy.

Consequently and in the frame of test cases investigated, it appears that the use of a multi-steps scheme with a finite difference evaluation of the $J_R \Delta Q^n$ product and coupled with GMRES algorithm (here named as scheme F) is the more efficient scheme and is thus recommended for viscous flow computations.

Conclusions

A computational investigation of the flow about the two-element Williams airfoil with either 10° and 30° flap deflection has been performed in inviscid and viscous incompressible turbulent flow conditions. Multiblock grids have been generated in a fully-automatic way using the object-oriented concept. Inviscid solutions at zero incidence were compared and found in good agreement with the Karman-Trefftz mapping method of Williams and the panel method of Coussement. However, slight discrepancies may be observed in C_p distributions, indicating a need for further grid refinement in the region of the gap. A comparison of the efficiency of seven different implicit strategies has been performed in the turbulent regime at zero incidence for Re = 1.2 million. Multi-steps schemes appears more efficient than single-step ones as far as the jacobians are approximated in an accurate way. In the frame of the test cases investigated, a 10-steps scheme coupled with a first-order forward evaluation of the $J_R \Delta Q^n$ product and further accelerated using the GMRES algorithm appears to be an efficient approach to solve viscous low Reynolds numbers flows around complex multi-element airfoils configurations on multiblock grids. However, it is expected that the domain should be divided in a minimum number of blocks because the implicit operators are expected to be more efficient when applied over a large domain. The impact of various grid topologies as well as alternative turbulence and transition models on accuracy and non-linear convergence behaviors should also be investigated in a future study.

References

[1] Fritz W., '*Calculation of Maximum and High Lift Characteristics of Multi-Element Airfoils*', In AGARD Conference Proceedings CP-515 on High Lift System Aerodynamics (1992).

[2] Bartsch P., Nitsche W., Britsch M., '*Navier-Stokes Computations of Turbulent Flow Around High-Lift Configurations*', In AGARD Conference Proceedings CP-515 on High Lift System Aerodynamics (1992).

[3] Rogers S., Menter F., Durbin P., Mansour N., '*A Comparison of Turbulence Models in Computing Multi-Element Airfoil Flows*', AIAA Paper 94-0291 (1994).

[4] Mathias D., Roth K., Ross J., Rogers S., Cummings R., '*Navier-Stokes Analysis of the Flow about a Flap Edge*', AIAA Paper 95-0185 (1995).

[5] Cao H., Kusunose K., '*Numerical Prediction of Reverse Reynolds Number Effects for Multi-Element Airfoils*', In Numerical Methods in Laminar and Turbulent Flows '95, Vol IX Part 1 pp 457-468, edited by C.Taylor and P.Durbetaki, Pineridge Press (1995).

[6] Barth T.J., '*Numerical Aspects of Computing Viscous High Reynolds Number Flows on Unstructured Meshes*', AIAA Paper 91-0721 (1991).

[7] Yu T.Z., Soni B.K., Shih M.H., '*CAGI : Computer Aided Grid Interface*', AIAA Paper 95-0243 (1995).

[8] Chorin A.J. , 'A Numerical Method for Solving Incompressible Viscous Flow Problems', Journal of Computational Physics, 2, pp 12-26 (1967).

[9] Baldwin B., Lomax H., '*Thin Layer Approximation and Algebraic Model for Separated Turbulent Flows*', AIAA Paper 78-25 (1978).

[10] Turner M., Jennions I., '*An Investigation of Turbulence Modeling in Transonic Fans Including a Novel Implementation of an Implicit k-ε Model*',

ASME Journal of Turbomachinery, Vol. 115 pp 249-260 (April 1993).

[11] Granville P., '*Baldwin-Lomax Factors for Turbulent Boundary-Layers in Pressure Gradient*', AIAA Journal, Vol.25(12), pp 1624-1627 (1987).

[12] Wilquem F., Degrez G., '*A Multiblock Strategy for the Solution of the 2D Incompressible Navier-Stokes Equations*', In Numerical Methods in Laminar and Turbulent Flows '95, Vol IX Part 2 pp 1185-1196, edited by C.Taylor and P.Durbetaki, Pineridge Press (1995).

[13] Jameson A., Yoon S., '*Lower-Upper Implicit Schemes with Multiple Grids for the Euler Equations*', AIAA Journal 25(7), pp 929-935 (1987).

[14] Issman E., Degrez G., '*Convergence Acceleration of a 2D Multiblock Euler Navier Stokes Solver*', von Karman Institute PR 1993-05 (1993).

[15] Saad Y., Schultz M.,'*GMRES : A Generalized Minimal Residual Algorithm for Solving Non-Symmetric Linear Systems*', SIAM Journal of Sci.Stat.Comput. Vol 7(3) pp 856-869 (1986).

[16] Williams B., '*An Exact Test Case for the Plane Potential Flow about Two Adjacent Lifting Airfoils*', RAE Report n°3717 (1971).

[17] Coussement G., '*Modélisation Numérique des Ecoulements Potentiels autour d'Obstacles par la Méthode des Panneaux*', Travail de Fin d'Etudes, Faculté Polytechnique de Mons (1988).